# Distribution patterns of 18F-fluorodeoxyglucose in large vessels of Takayasu's and giant cell arteritis using positron emission tomography

A. Soriano[1], G. Pazzola[1,5], L. Boiardi[1], M. Casali[2], F. Muratore[1,5], N. Pipitone[1], M. Catanoso[1], R. Aldigeri[3], L. Cimino[4], A. Versari[2], C. Salvarani[1,5]

*[1]Rheumatology Unit, [2]Nuclear Medicine Unit, Azienda USL, Istituto di Ricovero e Cura a Carattere Scientifico, Reggio Emilia, Italy; [3]Department of Medicine and Surgery, University of Parma, Italy; [4]Ophthalmology Unit, Azienda USL, Istituto di Ricovero e Cura a Carattere Scientifico, Reggio Emilia, Italy; [5]Università di Modena e Reggio Emilia, Italy.*

*Alessandra Soriano, MD*
*Giulia Pazzola, MD*
*Luigi Boiardi, MD, PhD*
*Massimiliano Casali, MD*
*Francesco Muratore, MD*
*Nicolò Pipitone, MD, PhD*
*Mariagrazia Catanoso, MD*
*Raffaella Aldigeri, MB*
*Luca Cimino, MD*
*Annibale Versari, MD*
*Carlo Salvarani, MD*

*Please address correspondence to:*
*Dr Carlo Salvarani,*
*Rheumatology Unit,*
*Arcispedale Santa Maria Nuova, IRCCS,*
*Viale Umberto I, 50,*
*42121 Reggio Emilia, Italy.*
*E-mail: carlo.salvarani@ausl.re.it*

*Received on December 16, 2017; accepted in revised form on April 16, 2018.*

*Clin Exp Rheumatol 2018; 36 (Suppl. 111): S99-S106.*



**Key words**: large vessel vasculitis, giant cell arteritis, Takayasu's arteritis, 18F-FDG PET/CT, cluster analysis, principal component analysis, distribution pattern

*Competing interests: N. Pipitone has received royalties from UCB, Alfa-Wassermann, Uptodate.com, Servier, GSK and funding from AIFA. All the other authors declare no competing interests.*

## ABSTRACT

**Objective.** *To compare patterns of vascular involvement using 18F-fluorodeoxyglucose-positron emission tomography computed tomography (FDG PET/CT) in patients with giant cell arteritis (GCA) and Takayasu's arteritis (TAK).*

**Methods.** *A total of 130 consecutive $^{18}$F-FDG PET/CT scans performed during the disease course for evaluating disease activity in 15 GCA and 13 TAK patients were retrospectively examined by two nuclear physicians blinded to clinical data. Standardised uptake values (SUVmax) in 14 vascular districts including all the aortic segments and the main tributaries were measured. The average SUVmax value for each vascular district was also calculated. Principal component analysis (PCA) and agglomerative hierarchical cluster analysis (CA) were used to explore distribution patterns of vascular FDG uptake.*

**Results.** *The aortic segments showed the highest SUV max values among the different districts in both GCA and TAK. SUV max values measured in the different districts were significantly higher in GCA compared to TAK, except for the axillary arteries. Regarding thoracic and abdominal aorta, ascending aorta and aortic arch had the highest correlation in both vasculitis ($p<0.0001$). CA confirmed that carotid, axillary, subclavian, iliac and femoral arteries clustered with their contralateral counterpart in both vasculitis. The 3 components of thoracic aorta clustered with abdominal aorta in TAK, while aortic arch clustered only with ascending aorta, and descending and abdominal aorta grouped together with iliac and femoral arteries in GCA. PCA analysis identified 3 different components for TAK and GCA explaining 72% and 71% of the total variance respectively in these two vasculitis. Confirming CA, a component including the entire aortic district was identified in TAK, but not in GCA. Similar results in PCA using averaged data were observed.*

**Conclusion.** *Strong similarities, but also a subtle skewing in terms of distribution patterns of arterial involvement assessed by SUVmax values were observed between GCA and TAK.*

## Introduction

According to the 2012 International Chapel Hill Consensus Conference on the nomenclature of Vasculitides (CHCC2012), large-vessel vasculitis (LVV) is defined as a vasculitis affecting large arteries – namely aorta and its major branches – of which giant cell arteritis (GCA) and Takayasu's arteritis (TAK) represent the two main forms (1). However, some issues still remain debated in the disease classification of LVV, namely whether or not they represent two nosological entities on the same spectrum of disease (2).

GCA has traditionally been considered a vasculitic process with a tropism for some epicranial arteries in subjects older than 50 years (3). Over the last two decades, it has become clear that extracranial involvement may occur in 29–83% of the cases (4-8), being localised at the aorta and its primary branches in about two thirds of cases (9-10). It has also been noticed that the1990 ACR criteria are inadequate to correctly classify patients with large-vessel GCA, who seem to have a lower rate of vision loss, higher relapse rate and greater corticosteroids requirements (10).

Classification of patients with LVV may be challenging in routine clinical practice, since GCA and TAK share many clinical and radiological fea-

tures. Large-vessel involvement may be detected in the absence of cranial symptoms, or in subjects aged between 40 and 50 years who are not included in the classification criteria for either condition. Furthermore, the use of new imaging techniques has unveiled the presence of LV involvement in patients with polymyalgia rheumatica (PMR), a condition strictly related to GCA, without cranial ischaemic manifestations (11, 12). 18F-fluorodeoxyglucose-positron emission tomography computed tomography (18F-FDG PET/CT) studies demonstrated that a third of patients with PMR without symptoms or signs of GCA had an occult large vessel involvement, in particular some patients had a predominat involvement of the arteries of the lower extremities, mainly the femoro-popliteal arteries (12-14).

Striking similarities in the distribution of arterial lesions led some authors to postulate that GCA and TAK might be part of the same disease spectrum (15).

The diagnostic performance of $^{18}$F-FDG PET/CT in the evaluation of LVV disease characterisation and extension, both at onset and in the follow-up, has been investigated with different and contrasting results (16-20). These discrepant results are due to different factors: first of all, there is no consensus on how to interpret and grade scans, moreover the effects of steroids on vascular FDG uptake over time are not well-understood and may have significant dampening effects, making the results of the different studies difficult to compare. In the absence of a standardised reading approach and gold standard parameters for the assessment of LVV arterial inflammation *via* $^{18}$F-FDG PET/CT, there is a great need to develop analytical methodologies useful to properly interpret the information derived from such studies, and possibly to unveil differences or similarities between TAK and GCA.

Latent class analysis has recently been used to investigate alternative ways to classify LVV in few angiographic studies, on the basis of distribution patterns of arterial lesions (9, 21, 22). Other classical techniques - such as principal component analysis (PCA) and cluster analysis (CA) - have not yet been applied to investigate the distribution patterns of LVV as assessed by $^{18}$F-FDG PET/CT.

The aim of our study was to investigate whether PCA and CA are useful in identifying distinct distribution patterns of LVV assessed through $^{18}$F-FDG PET/CT. We also investigated a correlation between maximum standardised uptake (SUVmax) values of the different districts in both groups to look for preferential associations between vascular beds and disease extension at the aorta level. To adjust for correlated data from repeated measurements, we also performed the statistical analyses on averaged data.

## Patients and methods

We performed a retrospective review of consecutive patients with LVV fulfilling the 1990 American College of Rheumatology (ACR) classification criteria for GCA and TAK (23, 24) who had been referred for $^{18}$F-FDG PET/CT scan during their follow-up at the Nuclear Medicine Unit of our hospital from January 2008 through December 2013. We included only patients who had at least 3 follow-up nuclear examinations.

As a tertiary reference centre for vasculitis, we admit patients with suspected, early or established LVV for re-evaluation of treatment and/or disease activity. We provide to patients with LVV a standardised yearly screening for a comprehensive evaluation of disease activity and extension by using duplex sonography, CT- or MR-angiography (CTA, MRA), and 18F-FDG PET/CT since 2008. This protocol includes determination of erythrocyte sedimentation rate (ESR) and C-reactive protein (CRP) at the time of $^{18}$F-FDG PET/CT evaluation. Kerr/NIH criteria and ITAS score are used to evaluate disease activity in TAK patients (25, 26).

Baseline demographic information including age, sex, race, as well as clinical signs and symptoms, date of diagnosis and disease duration, inflammatory markers [erythrocyte sedimentation rate, ESR, normal values 0-30 mm/h; C-reactive protein, CRP, normal values 0-0.5 mg/dL] repeatedly measured at the onset and during the follow-up, histopathological findings - in the case of GCA -, imaging study results and therapeutic schedules of the entire population were entered into an electronic database, starting from 2008.

Patients with a diagnosis of GCA underwent $^{18}$F-FDG PET / CT when there was a clinical suspicion for LVV and/or when CTA/MRA and duplex sonography demonstrated lumen changes or vascular thickening, respectively.

Both patients with large vessel (LV) GCA and TAK underwent repeat $^{18}$F-FDG PET/CT at follow-up on a yearly basis as part of a standard screening procedure. Additional 18F-FDG PET/CT exams could be requested in cases where the disease appeared active based on 1) clinical and laboratory parameters, or 2) the evidence of evolving vascular damage during follow-up imaging studies.

28 consecutive patients with LVV underwent a total of 130 $^{18}$F-FDG PET/CT studies during their follow-up period at the Nuclear Medicine Unit of our hospital from January 2008 through December 2013, with a median number of 4.6 $^{18}$F-FDG PET/CT studies per patient. 28 patients contributed to the analyses with 3 scans, 21 patients with 4, 17 patients with 5, 8 patients with 6, 3 patients with 7, and 2 patients with 8. Specifically, there were 15 patients with LV GCA (11 females, 4 males) and 13 patients with TAK (11 females, 2 males); mean age of the entire group (± SD) 48±15 years. Inflammatory markers (ESR, CRP) were recorded as long as they had been obtained no more than 2 weeks before $^{18}$F-FDG PET/CT. Corticosteroid dosage (prednisone, mg/day) and immunosuppressive treatment at imaging time were recorded.

The study was approved by the local Ethics Committee.

### *$^{18}$F-FDG PET/CT imaging protocol and analysis*

PET/CT data were acquired using a Discovery GE PET/CT scanner (General Electrics Medical Systems Cleveland, OH, USA), which combines a helical 16-slices CT and a 3-dimensional (3-D) PET scanner. Patients were scanned 60 minutes after the injection of 5 MBq/kg $^{18}$F-FDG.

CT helical scans without contrast-injection were acquired first (scan field 500 mm, increment 3.75 mm, slice thickness 3.75 mm, pitch 1, 0.8 seconds per rotation, matrix 512x512 pixels, 120 kV, 80 mA). PET scanning started at the end of CT transmission, and consisted of 8-11 bed positions of 3.3 minutes each. Total acquisition time per patient varied from 30 to 40 minutes.

Patients fasted four hours before PET/CT scan. Fasting blood glucose levels (before the injection of $^{18}$F-FDG) and activity of the injected $^{18}$F-FDG were recorded to insure comparability and resulted below 160 mg/dl in all patients.

$^{18}$F-FDG PET scan images were displayed in coronal, axial and sagittal planes and with rotating 3-D images. They were reviewed by two nuclear physicians (AV, MC) blinded to clinical and laboratory data. Visual analysis was performed in the following 14 vessel segments: ascending aorta, aortic arch, descending thoracic aorta, right carotid artery, left carotid artery, right subclavian artery, left subclavian artery, right axillary artery, left axillary artery, abdominal aorta, right iliac artery, left iliac artery, right femoral artery and left femoral artery.

Vascular uptake was graded using the maximum standardised uptake value (SUVmax), defined as the ratio of $^{18}$F-FDG activity to injected activity and normalised to body mass. Regions of interest (ROIs) in 3-D around the vessel wall in axial, sagittal and coronal slices were manually applied and the corresponding maximum SUV (SUVmax) was recorded. Fused PET/CT images allowed adequate ROI placement within the vessel and exclusion of adjacent structures. Representative SUVmax segmental values were calculated for each above-mentioned compartment.

*Statistical methods*

Continuous variables were described by mean ± standard deviation (SD) or median (interquartile range) and compared by *t* test or Mann-Whitney test, as appropriate. Categorical variables were reported by frequencies and compared by Chi-square test.

SUVmax in 14 vascular districts including aortic segments (ascending aorta, aortic arch, descending thoracic aorta and abdominal aorta) and the main tributaries (carotid, subclavian, axillary, iliac and femoral arteries; each bilaterally) were standardised through Z-score calculation.

To adjust for correlated data from repeated measurements, we calculated for each patient the average SUVmax value over successive examinations for each singular vascular district and we performed the statistical analyses, in particular CA and PCA, also on averaged data. These analyses are displayed in Supplementary Tables.

Correlation between SUVmax values and average SUVmax values of the different districts was determined by Spearman correlation test.

In order to analyse the distribution patterns of arterial involvement between the two main variants of LVV (TAK and GCA), we used two different exploratory approaches: CA (27) and PCA (28).

Agglomerative hierarchical clustering was performed, Euclidian distance was used to calculate the distance between clusters and Ward's method to agglomerate clusters. Two dendrograms were created. Each dendrogram corresponds to the tree diagram generated to illustrate the arrangement of the cluster.

PCA was used to reduce the number of variables onto a smaller number of new orthogonal variables, so-called Principal Components (PCs). Varimax rotation was used to extract the PCs because it maximises the sum of the vari-

**Table I.** Patient characteristics at the time of $^{18}$F-FDG PET/CT scans.

| | All (n=130) | TAK (n=60) | GCA (n=70) | *p* |
|---|---|---|---|---|
| Age, years | 48 ± 15 | 34 ± 8 | 60 ± 9 | <0.0001 |
| ESR, mm/h | 33.6 ± 28.5 | 30.5 ± 23.4 | 36.1 ± 32.2 | 0.55 |
| CRP, mg/dL | 1.58 ± 2.45 | 1.96 ± 3.0 | 1.23 ± 1.80 | 0.40 |
| Prednisone dosage, mg/day | 7.0 ± 6.4 | 6.5 ± 3.2 | 7.5 ± 10.6 | 0.75 |
| Prednisone, n (%) | 84 (65) | 35 (58) | 49 (70) | 0.13 |
| Immunosuppressants, n (%) | 91 (70) | 47 (77) | 44 (64) | 0.10 |
| Biologics, n (%) | 31 (24) | 16 (22) | 15 (22) | 0.55 |
| Kerr/NIH criteria ≥2*, n (%) | 16 (12) | 10 (17) | 6 (9) | 0.20 |
| Median disease duration, months | 36 (17-64) | 34 (16-59) | 40 (20-71) | 0.46 |
| Median follow-up, months | 42 (30-53) | 40 (32-49) | 49 (25-55) | 0.82 |

Mean values ± SD or median (IQR) and frequencies (%). TAK: Takayasu's arteritis; GCA: giant cells arteritis; ESR: erythrocyte sedimentation rate (normal values 0-30 mm/h); CRP: C-reactive protein (normal values 0-0.5 mg/dL).
*Kerr/NIH criteria ≥2 defines a state of active disease.

**Table II.** Comparison of maximum standardised uptake value (SUVmax) values in 14 vascular districts between Takayasu's arteritis and giant cell arteritis.

| Vascular district | Takayasu's arteritis (n=60) | Giant cell arteritis (n=70) | *p* |
|---|---|---|---|
| Right carotid artery | 1.60 (1.40-1.80) | 1.90 (1.60-2.32) | 0.03 |
| Left carotid artery | 1.60 (1.30-2.07) | 1.90 (1.60-2.40) | <0.0001 |
| Right subclavian artery | 1.50 (1.22-2.00) | 1.80 (1.57-2.20) | 0.002 |
| Left subclavian artery | 1.40 (1.10-2.00) | 1.90 (1.50-2.20) | 0.001 |
| Right axillary artery | 0.85 (0.60-1.20) | 0.90 (0.67-1.50) | 0.353 |
| Left axillary artery | 0.90 (0.70-1.27) | 1.00 (0.70-1.50) | 0.472 |
| Ascending aorta | 2.10 (1.70-2.70) | 2.70 (2.30-3.77) | <0.0001 |
| Aortic arch | 2.20 (1.82-2.60) | 2.70 (2.40-3.50) | <0.0001 |
| Descending aorta | 2.10 (1.72-2.60) | 2.50 (2.00-3.10) | 0.001 |
| Abdominal aorta | 1.85 (1.70-2.40) | 2.40 (1.87-2.90) | <0.0001 |
| Right iliac artery | 1.60 (1.30-1.87) | 1.80 (1.50-2.12) | 0.002 |
| Left iliac artery | 1.50 (1.30-1.70) | 1.70 (1.40-2.20) | <0.0001 |
| Right femoral artery | 1.30 (1.20-1.67) | 1.60 (1.37-2.00) | <0.0001 |
| Left femoral artery | 1.40 (1.10-1.60) | 1.70 (1.40-2.02) | <0.0001 |

Values are reported as median (IQR). NS: not significant.

ances of the squared coefficients within each eigenvector, and the rotated axes remain orthogonal. Eigenvalues greater than 1 were required to retain factors. The analysis revealed a set of three orthogonal factors sufficient to explain 70-72% of the total variance.

Kaiser-Meyer-Olkin (KMO) test of sampling adequacy and Bartlett's test of sphericity were computed to establish the validity of data set, at 1% level of significance.

Statistical analyses were carried out using SPSS statistics v. 24 (IBM Statistics, USA). The significance level was set at $p$=0.05.

*Ethical approval*

All procedures performed in studies involving human participants were in accordance with the ethical standards of the institutional and/or national research committee and with the 1964 Helsinki declaration and its later amendments or comparable ethical standards. For this type of study formal consent is not required.

## Results

*Patient characteristics*

Twenty-eight patients with LVV (GCA and TAK) underwent a total of 130 $^{18}$F-FDG PET/CT scans, n=60 for TAK and n=70 for GCA in a follow-up period of 6 years (2008-2013). The median disease duration at the time of the first PET/CT scan was 14 months for both TAK patients (IQR: 4–36 months) and GCA patients (IQR: 7–51 months) ($p$=1.00). Patient characteristics are displayed in Table I. The entire population was Caucasian. The two groups showed significant differences in age, but not in disease duration and laboratory parameters, nor in medium prednisone dosage at the time of the examination and in the frequencies of patients associating traditional immunosuppressants or biologic agents.

The mean value ± SD of ITAS score was 0.24±0.43 and of Kerr/NIH was 0.19±0.40 in the TAK group.

The aortic segments showed the highest values of SUVmax among the different districts in both diagnoses (Table II). However, the SUVmax values measured in the different districts were significantly higher in GCA as compared to TAK, except for the axillary arteries. Specifically, median (IQR) of SUVmax at ascending aorta (2.70 [2.30–3.77] *vs*. 2.10 [1.70–2.70], $p$<0.0001), aortic arch (2.70 [2.40–3.50] *vs*. 2.20 [1.82-2.60], $p$<0.0001), descending aorta (2.50 [2.00–3.10] *vs*. 2.10 [1.72–2.60], $p$=0.001) and abdominal aorta (2.40 [1.87–2.90] *vs*. 1.85 [1.70-2.40], $p$<0.0001) were significantly higher in GCA than TAK patients.

SUVmax value of each district showed a significant correlation with the others in the majority of the cases. The highest correlation among SUVmax values was observed with the contralateral arterial bed, with correlation coefficients ranging from 0.68 (iliac artery) to 0.85 (axillary artery) in TAK (Table III), and from 0.62 (subclavian artery) to 0.84 (axillary artery) in GCA (Table IV). Regarding the thoracic aorta and abdominal aorta, in TAK descending aorta and aortic arch had the highest correlation ($\varrho$ = 0.69, $p$<0.0001), while in GCA the highest correlation was observed between ascending aorta and aortic arch ($\varrho$ = 0.76, $p$<0.0001).

Supplementary Table 1 shows the comparison of average SUVmax values in 14 vascular districts between TA and GCA, and supplementary Tables 2 and 3 the vascular beds with highest correlation with any given artery (mean SUV max value of all scans for every segment for each patients) in TAK and GCA, respectively. Similar results were obtained.

*Hierarchical cluster analysis*

CA confirmed that carotid, axillary, subclavian, iliac, and femoral arteries clustered with their contralateral counterpart (Fig. 1) in both diagnoses. We observed different patterns in clustering for the two different vasculitis. In the TAK group we found three different clusters: (1) femoral and iliac cluster; (2) aortic arch, ascending, descending and abdominal aorta cluster; (3) carotid, subclavian and axillary cluster. In the GCA group we observed a cluster of axillary, subclavian and carotid districts. Aortic arch clustered only with ascending aorta, while descending and abdominal aorta grouped together with iliac and femoral arteries.

Also using averaged data, carotid, axillary, subclavian, iliac, and femoral arteries clustered with their contralateral counterpart (Supplementary Fig. 1).

**Table III.** Vascular beds with the highest correlation with any given artery in the 60 scans of the 13 patients with Takayasu's arteritis*.

| Artery | Involvement best correlating with | $\varrho$ | $p$ |
|---|---|---|---|
| Aortic arch | Descending aorta | 0.689 | <0.0001 |
| Ascending aorta | Aortic arch | 0.661 | <0.0001 |
| Abdominal aorta | Right femoral artery | 0.546 | <0.0001 |
| Right carotid artery | Left carotid artery | 0.839 | <0.0001 |
| Right iliac artery | Left iliac artery | 0.682 | <0.0001 |
| Right subclavian artery | Left sublavian artery | 0.707 | <0.0001 |
| Right axillary artery | Left axillary artery | 0.850 | <0.0001 |
| Right femoral artery | Left femoral artery | 0.715 | <0.0001 |

*The correlation coefficient and $p$-value are for simultaneous involvement of the two indicated arteries.

**Table IV.** Vascular beds with the highest correlation with any given artery in the 70 scans of the 15 patients with giant cell arteritis*.

| Artery | Involvement best correlating with | $\varrho$ | $p$ |
|---|---|---|---|
| Aortic arch | Ascending aorta | 0.765 | <0.0001 |
| Descending aorta | Abdominal aorta | 0.692 | <0.0001 |
| Right carotid artery | Left carotid artery | 0.720 | <0.0001 |
| Right iliac artery | Left iliac artery | 0.708 | <0.0001 |
| Right subclavian artery | Left sublavian artery | 0.619 | <0.0001 |
| Right axillary artery | Left axillary artery | 0.838 | <0.0001 |
| Right femoral artery | Left femoral artery | 0.819 | <0.0001 |

*The correlation coefficient and $p$-value are for simultaneous involvement of the two indicated arteries.

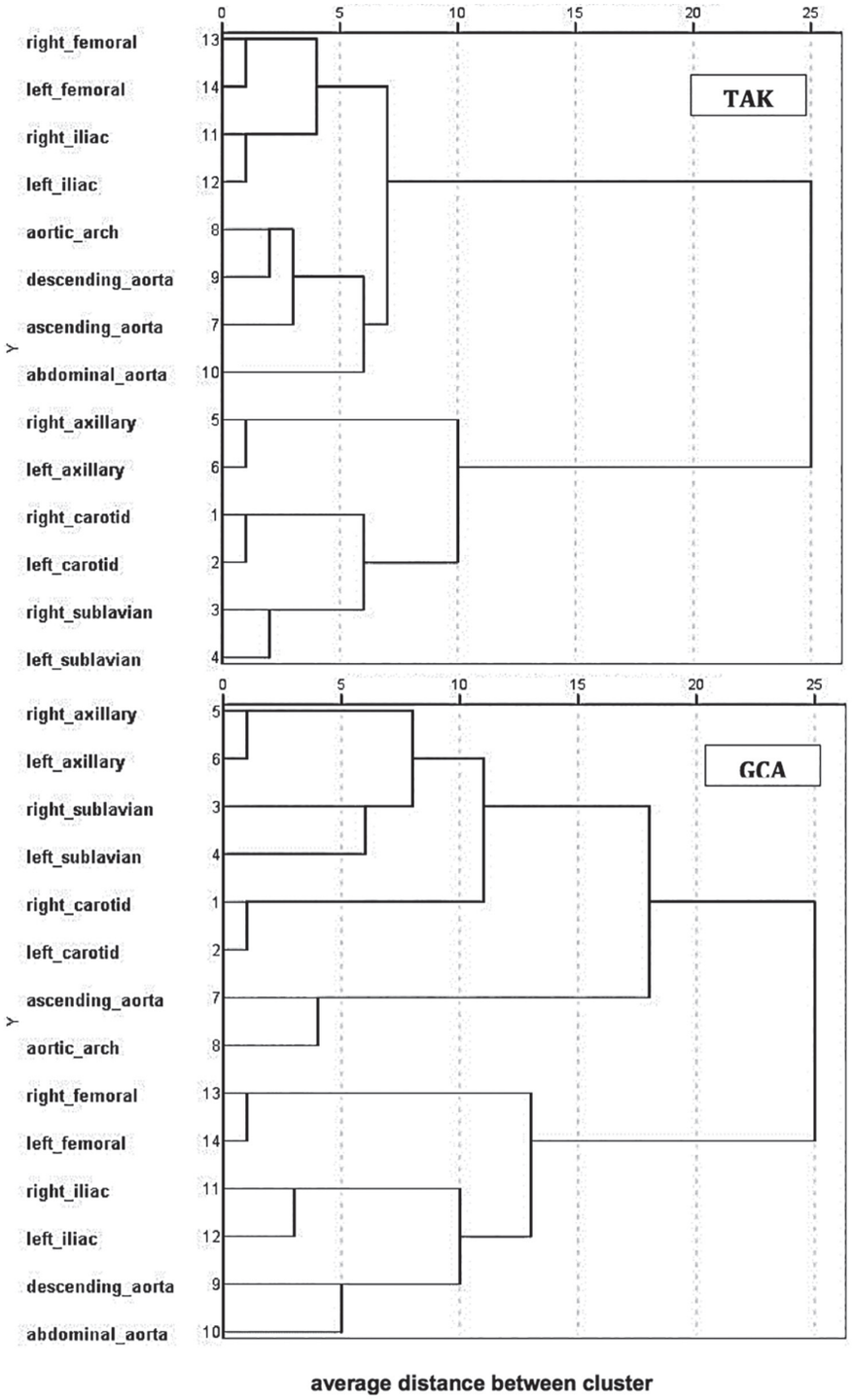


**Fig. 1.** Cluster patterns in Takayasu's arteritis (TAK) and giant cell arteritis (GCA) patients.

*Principal component analysis*

PCA applied on the original 14 variables revealed three different orthogonal components that accounted for 72% and 71% of the total variance in TAK and GCA, respectively. The first component accounted for 45% of the variance in TAK diagnosis and 47% in GCA diagnosis. The Kaiser-Meyer-Olkin (KMO) analysis was performed, yielding an index of 0.77 and 0.79. The result for Bartlett's test of sphericity was highly significant in both cases ($p$<0.0001). These results confirmed the appropriateness of PCA.

Similarly to CA, PCA showed a different composition of the three PCs for GCA and TAK group. In TAK we observed a first component incorporating carotid, subclavian and axillary arteries; a second component characterised by iliac and femoral vascular districts; and a third one described by aortic thoracic segments and abdominal aorta. In a different way, PCA of the GCA group identified a first component incorporating iliac, femoral arteries, abdominal and descending aorta, a second one characterised by axillary, carotid and subclavian arteries; and a third component including ascending aorta and aortic arch (Table V).

Supplementary Table 4 shows PCA using averaged data. The results were similar. Three different PCs that accounted for 86% and 79% of the total variance in TAK and GCA were observed. The same different composition of the three PCs for GCA and TAK groups was present.

## Discussion

We decided to perform hierarchical CA primarily to find out possible differences between GCA and TAK (*i.e.*, delineation of subgroups) studied by $^{18}$F-FDG PET/CT. Using 18F-FDG PET/CT, we confirmed similar patterns of arterial involvement in GCA and TAK patients. We found that in both conditions the arterial involvement was symmetric in paired vessels and contiguous in the aorta. However, some differences were also observed. CA revealed three different components in GCA and TAK, which differed in terms of inclusion of the entire aorta segments in TAK and not in GCA, where abdominal aorta and descending aorta clustered with iliac and femoral arteries. Ascending aorta and aortic arch clustered separately in GCA. Being CA considered very efficient but with a tendency in producing small size clusters, PCA was additionally performed to confirm data. Analogously, we observed a difference in TAK and GCA groups at the same level. A second observed difference in PCA between GCA and TAK groups was related to the different arterial disease patterns explaining the largest portion of the total variance (supra-aortic vessels in TAK and descending and abdominal aorta, and iliac and femoral arteries in GCA). This suggests a

different extension of the vascular involvement during the follow-up and under the influence of immunosuppressive treatment.

To adjust for correlated data from repeated measurements, we calculated for each patient the average SUV value over successive examinations for each single vascular district and we performed PCA on averaged data. No differences in the results were observed.

Evidence from the literature about the usefulness of CA as statistical method in the evaluation of pattern distribution of vascular lesions in LVV is scarce and comes from few studies performed with different imaging techniques, not including $^{18}$F-FDG PET/CT (9, 21, 22). Arnaud *et al*. (21) previously used agglomerative hierarchical CA to investigate patterns of arterial involvement in a population of 82 TAK patients studied by peripheral vascular Doppler, CT and MR angiography.

The study revealed symmetric distribution in paired vascular territories of TAK lesions, while they had contiguous extension in the aorta territory. In particular, with the exception of internal and external carotid arteries all paired arterial beds clustered with their contralateral counterpart.

Similarly to our findings, in their study the entire thoracic districts clustered together with the abdominal aorta, suggesting contiguous involvement in these territories (21).

Contiguous arterial involvement in the aorta and usually symmetric involvement in paired branch vessels in both TAK and GCA was also found by Grayson *et al*. (9), who used latent class analysis to analyse data from MR angiography studies of two different North American LVV cohorts. Thoracic aorta most strongly correlated with the abdominal aorta in both groups in their study. Carotid and mesenteric arterial disease, as well as left subclavian disease, were seen more frequently in TAK; conversely, axillary disease was more frequently observed in GCA, in association with a concomitant symmetric subclavian involvement (9).

In our study, SUVmax value of each district showed a significant correlation with the others in the majority of the cases in both conditions. Furthermore, similarly to Grayson *et al*., we observed in TAK and GCA patients a correlation and clustering between thoracic aorta and abdominal aorta. However, while in TAK abdominal aorta clustered more closely with all three components of thoracic aorta, in GCA descending aorta and abdominal aorta clustered more closely with iliac and femoral arteries than with ascending aorta and aortic arch. The contiguous modality of disease extension at the aorta level was then confirmed in our study in both vasculitis.

We also observed a symmetric extension of the lesions in paired vascular beds at carotid, subclavian, axillary, iliac and femoral arteries in the entire population of LVV. The highest correlation among SUVmax values was observed with the contralateral arterial bed.

Our data on the absence of significant differences in the SUVmax values in both axillary arteries between GCA and TAK seem to be in contrast with some previous findings by Grayson *et al*. (9), which revealed an increased prevalence of axillary involvement in GCA patients. These authors also reported an increased frequency of left subclavian artery involvement and an asymmetric clustering of subclavian disease in TAK. Similarly to Arnaud *et al*. (21), in our study subclavian disease clustered in TAK symmetrically as in GCA.

Although medium daily dosage of prednisone and mean levels of inflammatory markers at imaging time were comparable in the two groups, the comparison between SUVmax values in 14 selected vascular districts in patients with TAK and GCA, respectively, revealed significantly higher values in the latter, especially at the aorta level, with the only exception of the axillary arteries. Although no firm conclusions can be drawn from these data, they are intriguing because the higher 18-F-FDG uptake in almost all vascular beds observed in GCA compared to TAK - despite the lack of clinical activity in most patients - may be construed as evidence of a more persistent active disease in GCA during the disease course even under immunosuppressive treatment. Evidence supporting a persistent disease activity at the histopathological level in GCA during GC treatment came from a recent prospective follow-up study on temporal artery biopsies (29).

We found no correlation between SUVmax values and age population in GCA (data not shown), which might suggest that the higher arterial SUVmax in GCA compared to TAK might be related to the disease itself and its mechanisms, rather than to concomi-

**Table V.** Principal component analysis (PCA) results in Takayasu's arteritis (TAK) and giant cell arteritis (GCA).

| | TAK | | | GCA | | |
|---|---|---|---|---|---|---|
| | PC1 | PC2 | PC3 | PC1 | PC2 | PC3 |
| Explained variance % | 45.3 | 18.3 | 8.7 | 46.6 | 14.4 | 9.6 |
| Right carotid artery | 0.868 | 0.094 | 0.224 | 0.297 | 0.676 | 0.222 |
| Left carotid artery | 0.824 | 0.243 | 0.220 | 0.181 | 0.605 | 0.379 |
| Right subclavian artery | 0.775 | 0.194 | 0.396 | 0.355 | 0.498 | 0.524 |
| Left subclavian artery | 0.805 | 0.058 | 0.319 | 0.148 | 0.617 | 0.302 |
| Right axillary artery | 0.907 | 0.092 | 0.023 | 0.096 | 0.911 | 0.028 |
| Left axillary artery | 0.870 | 0.082 | -0.017 | 0.118 | 0.879 | -0.054 |
| Ascending aorta | 0.217 | 0.166 | 0.720 | 0.066 | 0.153 | 0.880 |
| Aortic arch | 0.132 | 0.264 | 0.848 | 0.373 | 0.127 | 0.818 |
| Descending aorta | 0.087 | 0.218 | 0.775 | 0.721 | 0.324 | 0.392 |
| Abdominal aorta | 0.180 | 0.187 | 0.476 | 0.633 | 0.338 | 0.160 |
| Right iliac artery | 0.044 | 0.865 | 0.186 | 0.856 | 0.159 | 0.016 |
| Left iliac artery | 0.167 | 0.828 | 0.136 | 0.903 | 0.129 | 0.002 |
| Right femoral artery | 0.253 | 0.745 | 0.363 | 0.748 | 0.172 | 0.324 |
| Left femoral artery | 0.086 | 0.806 | 0.306 | 0.781 | 0.036 | 0.355 |

tant immunosenescence-related processes and atherosclerosis. In general, TAK has a prolonged and indolent course with a significant delay in the diagnosis, as compared to GCA (30). We cannot exclude that the longer time to diagnosis of TAK may have influenced our results.

The current study has several limitations. Its retrospective nature is one of the main limitation, however it was balanced by the fact that our patients were homogeneously followed up at a single centre with a standardised yearly screening procedure. In GCA patients, 18F-FDG PET/CT was performed only when there was a clinical suspicion of LVV, therefore a selection bias toward GCA patients with a vascular disease pattern more similar to that of TAK is highly probable. Moreover, the use of immunosuppressive drugs by an elevated number of patients and differences in the disease duration might have interfered with imaging results. Additionally, it is unclear whether persistent vascular low-grade FDG uptake in treated patients considered to be in remission represents vascular remodelling or smoldering arterial wall inflammation, PET/CT may not be able to fully represent the vascular inflammatory process in comparison with histology as the gold standard.

Furthermore, there is only very limited evidence linking mural and luminal changes detected by CT and MRI/ MR angiography, on the one hand, and increased 18F-FDG uptake values in the same districts, on the other. Therefore the comparison between the results of studies using different imaging techniques remains challenging, despite the same statistical analysis used.

The strength of the study consists in having selected a homogeneous LVV population, entirely constituted by Caucasian subjects, with similar levels of inflammatory markers, without significant differences in terms of therapeutic schedules, followed-up at a single tertiary centre. The number of consecutive 18F-FDG PET/CT studies is large and the methodological approach included sophisticated analytic techniques for comparing complex patterns of arterial disease in TAK and GCA.

To our knowledge, this is the first study using the statistical approach of hierarchical CA and PCA to compare consecutive 18F-FDG PET/CT findings in a population of LVV patients in order to unveil preferential patterns of arterial involvement in GCA and TAK.

Our study showed similar distribution pattern of the arterial lesions in the two main variants of LVV, although some subtle differences were also observed, confirming that TAK and GCA are not two different conditions but part of the same disease spectrum. The quantitative analysis of 18F-FDG PET/CT data (SUV max values) confirmed the tendency of arterial lesions to be contiguous in the aorta and symmetric in branch vessels, as previously observed in angiographic studies. The distribution modalities of affected vessels appeared similar to previous evidence with few exceptions, and despite the different imaging technique used.

We have also shown for the first time a symmetric extension of the lesions in paired vascular beds at carotid, axillary, subclavian, iliac and femoral arteries level, clustering with the contralateral counterpart not only in TAK but also in GCA population.

A careful evaluation of the controlateral artery may be useful for improving the radiological follow-up of patients with LVV.

Further studies are needed to elucidate the diagnostic performance of 18F-FDG PET/CT in the follow-up of LVV patients and the role of atherosclerosis and immunosenescence in the LV-GCA.

## References


1. JENNETTE JC, FALK RJ, BACON PA *et al*.: Revised International Chapel Hill Consensus Conference Nomenclature of Vasculitides, *Arthritis Rheum* 2013; 65: 1-11.
2. GRAYSON P: Lumpers and splitters: ongoing issues in the classification of large vessel vasculitis, *J Rheumatol* 2015; 42: 149-51.
3. SALVARANI C, PIPITONE N, VERSARI A, HUNDER GG: Clinical features of polymyalgia rheumatica and giant cell arteritis. *Nat Rev Rheumatol* 2012; 8: 509-21.
4. BLOCKMANS D, DE CEUNINCK L, VANDERSCHUEREN S, KNOCKAERT D, MERTELMANS L, BOBBAERS H: Repetitive 18-fluorodeoxyglucose positron emission tomography in giant cell arteritis: study of 35 patients. *Arthritis Rheum* 2006; 55: 131-7.
5. SCHMIDT WA, SEIFERT A, GROMNICA-IHLE E, KRAUSE A, NATUSCH A: Ultrasound of proximal upper extremities arteries to increase the diagnostic yield in large-vessel giant cell arteritis. *Rheumatology* (Oxford) 2008; 47: 96-101.
6. ASCHWANDEN M, KESTEN F, STERN M *et al*.: Vascular involvement in patients with giant cell arteritis determined by duplex sonography of 2 x 11 arterial regions. *Ann Rheum Dis* 2010; 69: 1356-9.
7. PRIETO-GONZALEZ S, ARGUIS P, GARCIA-MARTINEZ A *et al*.: Large vessel involvement in biopsy-proven giant cell arteritis: prospective study in 40 newly diagnosed patients using CT angiography. *Ann Rheum Dis* 2012; 71: 1170-6.
8. GHINOI A, PIPITONE N, NICOLINI A *et al*.: Large-vessel involvement in recent-onset giant cell arteritis: a case-control colour-Doppler sonography study. *Rheumatology* (Oxford) 2012; 51: 730-4.
9. GRAYSON PC, MAKSIMOWICZ-MCKINNON K, CLARK TM *et al*.: Distribution of arterial lesions in Takayasu's arteritis and giant cell arteritis. *Ann Rheum Dis* 2012; 71: 1329-34.
10. MURATORE F, KERMANI TA, CROWSON CS *et al*.: Large-vessel giant cell arteritis: a cohort study. *Rheumatology* (Oxford) 2015; 54: 463-470.
11. SALVARANI C, CANTINI F, HUNDER GG: Polymyalgia rheumatica and giant-cell arteritis. *Lancet* 2008; 372: 234-45.
12. GONZÁLEZ-GAY MA, MATTESON EL, CASTAÑEDA S: Polymyalgia rheumatica. *Lancet* 2017; 390: 1700-12.
13. LORICERA J, BLANCO R, HERNÁNDEZ JL *et al*.: Non-infectious aortitis: a report of 32 cases from a single tertiary centre in a 4-year period and literature review. *Clin Exp Rheumatol* 2015; 33 (Suppl. 89): S-19-31.
14. GERMANÒ G, VERSARI A, MURATORE F *et al*.: Isolated vasculitis of the lower extremities in a patient with polymyalgia rheumatica and giant cell arteritis. *Clin Exp Rheumatol* 2011; 29 (Suppl. 64): S138-9.
15. MAKSIMOWICZ-MCKINNONK, CLARK TM, HOFFMAN GS: Takayasu arteritis and giant cell arteritis: a spectrum within the same disease? *Medicine* (Baltimore) 2009; 88: 221-6.
16. BLOCKMANS D, STROOBANTS S, MAES A, MORTELMANS L: Positron emission tomography in giant cell arteritis and polymyalgia rheumatic: evidence for inflammation of the aortic arch. *Am J Med* 2000; 108: 246-9.
17. PAPATHANASIOU ND, DU Y, MENEZES LJ *et al*.: 18F-fludeoxyglucose PET/CT in the evaluation of large-vessel vasculitis: diagnostic performance and correlation with clinical and laboratory parameters. *Br J Radiol* 2012; 85: e188-194.
18. BLOCKMANS D: Use of FDG-PET scan for the assessment of large vessel vasculitis. *Curr Treat Options in Rheum* 2016; 2: 153-60.
19. SALVARANI C, SORIANO A, MURATORE F, SHOENFELD Y, BLOCKMANS D: Is PET/CT essential in the diagnosis and follow-up of temporal arteritis? *Autoimmun Rev* 2017; 16: 1125-30.
20. MARTÍNEZ-RODRÍGUEZ I, JIMÉNEZ-ALONSO M, QUIRCE R *et al*.: $^{(18)}$F-FDG PET/CT in the follow-up of large-vessel vasculitis: A study of 37 consecutive patients. *Semin Arthritis Rheum* 2018; 47: 530-7.

21. ARNAUD L, HAROCHE J, TOLEDANO D *et al*.: Cluster analysis of arterial involvement in Takayasu arteritis reveals symmetric extension of the lesions in paired arterial beds. *Arthritis Rheum* 2011; 63: 1136-40.
22. FURUTA S, COUSINS C, CHAUDHRY A, JAYNE D: Clinical features and radiological findings in large vessel vasculitis: are Takayasu arteritis and giant cell arteritis two different diseases or a single entity? *J Rheumatol* 2015; 42: 300-8.
23. AREND WP, MICHEL BA, BLOCH DA *et al*.: The American College of Rheumatology 1990 criteria for the classification of Takayasu arteritis. *Arthritis Rheum* 1990; 33: 1129-34.
24. HUNDER GG, BLOCH DA, MICHEL BA *et al*.: The American College of Rheumatology 1990 criteria for the classification of giant cell arteritis. *Arthritis Rheum* 1990; 33: 1122-8.
25. KERR GS, HALLAHAN CW, GIORDANO J *et al*.: Takayasu arteritis. *Ann Intern Med* 1994; 120: 919-29.
26. MISRA R, DANDA D, RAJAPPA SM *et al*.: Development and the initial validation of the Indian Takayasu Clinical Activity Score (ITAS2010). *Rheumatology* (Oxford) 2013; 52: 795-801.
27. MASSART DL, KAUFMAN L: The Interpretation of Analytical Chemical Data by the Use of Cluster Analysis. John Wiley & Sons, New York, 1983.
28. JOLLIFFE IT: Principal Component Analysis. Springer, New York, 2002.
29. MALESZEWSKI JJ, YOUNGE BR, FRITZLEN JT *et al*.: Clinical and pathological evolution of giant cell arteritis: a prospective study of follow-up temporal artery biopsies in 40 treated patients. *Mod Pathol* 2017; 30: 788-96.
30. KERMANI TA, CROWSON CS, MURATORE F, SCHMIDT J, MATTESON EL, WARRINGTON KJ: Extra-cranial giant cell arteritis and Takayasu arteritis: How similar are they? *Semin Arthritis Rheum* 2015; 44: 724-8.